
HOKKAIDO UNIVERSITY

Title	Finite-Element Formulation in Terms of the Electric-Field Vector for Electromagnetic Waveguide Problems
Author(s)	Koshiba, M.; Hayata, K.; Suzuki, M.
Citation	IEEE Transactions on Microwave Theory and Techniques, 33(10), 900-905
Issue Date	1985-10
Doc URL	http://hdl.handle.net/2115/6037
Rights	©1985 IEEE. Personal use of this material is permitted. However, permission to reprint/republish this material for advertising or promotional purposes or for creating new collective works for resale or redistribution to servers or lists, or to reuse any copyrighted component of this work in other works must be obtained from the IEEE. IEEE, IEEE Transactions on Microwave Theory and Techniques, 33(10), 1985, p900-905
Type	article
File Information	ITMTT33_10.pdf


Instructions for use

Hokkaido University Collection of Scholarly and Academic Papers : HUSCAP

Finite-Element Formulation in Terms of the Electric-Field Vector for Electromagnetic Waveguide Problems

MASANORI KOSHIBA, SENIOR MEMBER, IEEE, KAZUYA HAYATA, AND MICHIO SUZUKI, SENIOR MEMBER, IEEE

Abstract—**A vector finite-element method for the analysis of anisotropic waveguides with off-diagonal elements in the permeability tensor is formulated in terms of all three components of the electric field. In this approach, spurious, nonphysical solutions do not appear anywhere above the "air-line." The application of this finite-element method to waveguides with an abrupt discontinuity in the permittivity is discussed. In particular, we discuss how to use the boundary conditions of the electric field at the interface between two media with different permittivities. To show the validity and usefulness of this formulation, examples are computed for dielectric-loaded waveguides and ferrite-loaded waveguides.**

I. Introduction

THE VECTOR finite-element method is widely used either in an axial-component ($E_z - H_z$) formulation [1]–[4] or in a three-component (either the electric field $\boldsymbol{E}$ or the magnetic field $\boldsymbol{H}$) formulation [5], [6], which enables one to compute accurately the mode spectrum of an electromagnetic waveguide with arbitrary cross section. The most serious difficulty in using the vector finite-element analysis is the appearance of spurious, nonphysical solutions [1]–[6]. Hano [7] has presented a three-component finite-element formulation with rectangular elements. In his formulation, spurious solutions, except for zero eigenvalues, do not appear, but a diagonal permittivity tensor and a diagonal permeability tensor are assumed. Recently, an improved finite-element method with triangular elements has been formulated for the analysis of anisotropic dielectric waveguides in terms of all three components of $\boldsymbol{H}$ [8]–[11]. In dielectric waveguides, the permeability is always assumed to be that of free space. Therefore, each component of $\boldsymbol{H}$ is continuous in the whole region and it is more advantageous to solve for $\boldsymbol{H}$ than for $\boldsymbol{E}$ [12]. In this improved $\boldsymbol{H}$-field formulation, no spurious solutions appear anywhere above the "air-line" corresponding to $\beta/k_0 = 1$ in a β/k_0 versus k_0 diagram [11], where k_0 is the wavenumber of free space and β is the phase constant in the z-direction. The appearance of spurious solutions is limited to the region $\beta/k_0 < 1$ and these solutions are equivalent to the TE modes of "hollow" waveguides [11]. The $\boldsymbol{H}$-field formulation is valid for general anisotropic waveguides with a nondiagonal permittivity tensor. However, it is difficult to apply this $\boldsymbol{H}$-field formulation to waveguides containing anisotropic media such as ferrites, because the tensor permeability may vary from material to material. In such cases, it is advantageous to solve for $\boldsymbol{E}$ rather than for $\boldsymbol{H}$.

In this paper, an improved finite-element method with triangular elements is formulated for the analysis of anisotropic waveguides with a nondiagonal permeability tensor using all three components of $\boldsymbol{E}$. In ferrite-loaded waveguides, the permittivity is assumed to be constant in each material, but may vary from material to material. At an abrupt discontinuity in the permittivity, there is an abrupt change in $\boldsymbol{E}$. In this work, the application of the $\boldsymbol{E}$-field formulation to waveguides with abrupt discontinuities in the permittivity is discussed in detail. In particular, we discuss how to use the boundary conditions of $\boldsymbol{E}$ at the interface between two media with different permittivities. In this improved $\boldsymbol{E}$-field formulation, no spurious solutions appear anywhere above the "air-line." The appearance of spurious solutions is limited to the region $\beta/k_0 < 1$ and these solutions are equivalent to the TM modes of "hollow" waveguides. To show the validity and usefulness of this formulation, examples are computed for dielectric-loaded waveguides and ferrite-loaded waveguides.

II. Functional Formulation

We consider an anisotropic waveguide with a tensor permeability and a scalar permittivity. With a time dependence of the form $\exp(j\omega t)$ being implied, Maxwell's equations are

$$\nabla \times \boldsymbol{E} = -j\omega\mu_0[\mu_r]\boldsymbol{H} \tag{1}$$

$$\nabla \times \boldsymbol{H} = j\omega\epsilon_0\epsilon_r\boldsymbol{E} \tag{2}$$

where ω is the angular frequency, μ_0 and ϵ_0 are the permeability and permittivity of free space, respectively, $[\mu_r]$ is the relative permeability tensor, $[\cdot]$ denotes a matrix, and ϵ_r is the relative permittivity which is assumed to be constant in each material.

From (1) into (2), the following wave equation is derived:

$$\nabla \times \left([\mu_r]^{-1}\nabla \times \boldsymbol{E}\right) - k_0^2\epsilon_r\boldsymbol{E} = 0 \tag{3}$$

Manuscript received February 1, 1985; revised May 22, 1985.

The authors are with the Department of Electronic Engineering, Hokkaido University, Sapporo, 060, Japan

0018-9480/85/1000-0900$01.00 ©1985 IEEE

where

$$k_0^2 = \omega^2 \epsilon_0 \mu_0. \tag{4}$$

The functional [12], [13] for (3) is known to be

$$F = \iint_\Omega (\nabla \times \boldsymbol{E})^* \cdot \left([\mu_r]^{-1} \nabla \times \boldsymbol{E}\right) d\Omega - k_0^2 \iint_\Omega \epsilon_r \boldsymbol{E}^* \cdot \boldsymbol{E}\, d\Omega \tag{5}$$

where Ω represents the cross section of the waveguide and the asterisk denotes complex conjugation. In the finite-element analysis using (5), spurious solutions appear scattered all over the propagation diagram [5]–[12], [14], [15]. These spurious solutions belong to two distinct categories [11], [14]. The first one (S_1) can be characterized as follows:

$$\nabla \times \boldsymbol{E} = 0 \quad \nabla \cdot \epsilon_r \boldsymbol{E} \neq 0 \qquad \text{for } k_0^2 = 0. \tag{6}$$

The second group (S_2) can be characterized as follows:

$$\nabla \times \boldsymbol{E} \neq 0 \quad \nabla \cdot \epsilon_r \boldsymbol{E} \neq 0 \qquad \text{for } k_0^2 > 0. \tag{7}$$

In order to eliminate the spurious solutions S_1 and S_2, we propose the following functional according to the $\boldsymbol{H}$-field formulation [8]–[11]:

$$\tilde{F} = \iint_\Omega (\nabla \times \boldsymbol{E})^* \cdot \left([\mu_r]^{-1} \nabla \times \boldsymbol{E}\right) d\Omega - k_0^2 \iint_\Omega \epsilon_r \boldsymbol{E}^* \cdot \boldsymbol{E}\, d\Omega + \iint_\Omega \epsilon_r^{-1} (\nabla \cdot \epsilon_r \boldsymbol{E})^* (\nabla \cdot \epsilon_r \boldsymbol{E})\, d\Omega. \tag{8}$$

For the functional (8), the first variation $\delta\tilde{F}$ is given by

$$\delta\tilde{F} = \iint_\Omega \delta \boldsymbol{E}^* \cdot \left[\nabla \times \left([\mu_r]^{-1} \nabla \times \boldsymbol{E}\right) - \nabla(\nabla \cdot \epsilon_r \boldsymbol{E}) - k_0^2 \epsilon_r \boldsymbol{E}\right] d\Omega - \int_\Gamma \delta \boldsymbol{E}^* \cdot \left[\boldsymbol{n} \times \left([\mu_r]^{-1} \nabla \times \boldsymbol{E}\right) - \boldsymbol{n}(\nabla \cdot \epsilon_r \boldsymbol{E})\right] d\Gamma \tag{9}$$

where Γ represents the contour of the region Ω, $\boldsymbol{n}$ is the outward unit normal vector to Γ, and the term $\boldsymbol{n} \times ([\mu_r]^{-1} \nabla \times \boldsymbol{E})$ corresponds to the tangential components of the magnetic field $\boldsymbol{H}$ on Γ. The stationary requirement $\delta\tilde{F} = 0$ yields

$$\nabla \times \left([\mu_r]^{-1} \nabla \times \boldsymbol{E}\right) - \nabla(\nabla \cdot \epsilon_r \boldsymbol{E}) - k_0^2 \epsilon_r \boldsymbol{E} = 0 \tag{10a}$$

as the Euler equation and

$$\boldsymbol{n}(\nabla \cdot \epsilon_r \boldsymbol{E}) = 0 \qquad \text{on perfect electric conductor} \tag{10b}$$

$$\boldsymbol{n} \times \left([\mu_r]^{-1} \nabla \times \boldsymbol{E}\right) = 0 \qquad \text{on perfect magnetic conductor} \tag{10c}$$

as natural boundary conditions, since $\delta\boldsymbol{E}^*$ in (9) is arbitrary. The spurious solutions S_1 and S_2 are not included in (8), but (8) may have other solutions than (3). This new group (S_3), characterized by

$$\nabla \times \boldsymbol{E} = 0 \quad \nabla \cdot \epsilon_r \boldsymbol{E} \neq 0 \qquad \text{for } k_0^2 > 0 \tag{11}$$

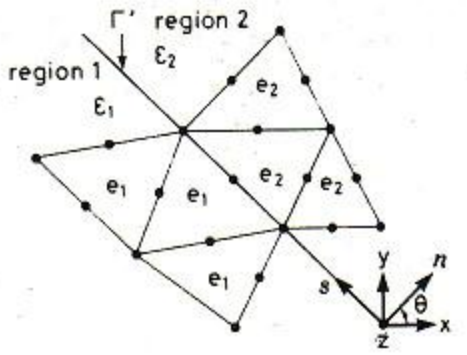

Fig. 1. Interface with an abrupt discontinuity in the permittivity.

obey the following equations:

$$\epsilon_r \boldsymbol{E} = \nabla \psi \tag{12a}$$

$$\left(\nabla^2 + k_0^2\right)\psi = 0 \text{ in region } \Omega \tag{12b}$$

$$\psi = 0 \text{ on perfect electric conductor} \tag{12c}$$

$$\partial\psi/\partial n = 0 \text{ on perfect magnetic conductor} \tag{12d}$$

where ψ is the scalar field. The electric field $\boldsymbol{E}$ of (12) satisfies the stationary requirement $\delta\tilde{F} = 0$, but the divergence of $\epsilon_r \boldsymbol{E}$ is not zero. Therefore, in the finite-element analysis using (8), spurious solutions S_3, which are not included in (5), do appear. The solutions S_3 are equivalent to the TM modes of "hollow" waveguides (replace ψ in (12b)–(12d) with E_z) and the appearance is limited to the region $\beta/k_0 < 1$. They do not appear anywhere above the "air-line."

III. Finite-Element Discretization and Boundary Conditions

Dividing the cross section Ω of the waveguide into a number of second-order triangular elements as shown in Fig. 1 and using the finite-element method on (8), we can write the functional for the whole region Ω in the form

$$\tilde{F} = \sum_e \tilde{F}_e \tag{13}$$

$$\tilde{F}_e = \{E\}_e^T [A]_e \{E\}_e \tag{14}$$

$$[A]_e = [S]_e + [U]_e - k_0^2 [T]_e \tag{15}$$

where $\{E\}_e$ is the electric-field vector corresponding to the nodal points within each element, the matrices $[S]_e$, $[T]_e$, and $[U]_e$ for each element are related to the first, second, and third terms on the right-hand side of (8), respectively, T, $\{\cdot\}$, and $\{\cdot\}^T$ denote a transpose, a column vector, and a row vector, respectively, and the summation Σ_e extends over all different elements. Variation of (13) with respect to the nodal variables leads to the eigenvalue problem.

In (14), the nodal electric-field vector $\{E\}_e$ should be forced to satisfy the boundary conditions at the interface between two media with different permittivities. We consider the interface Γ' with an abrupt discontinuity in the permittivity as shown in Fig. 1, where ϵ_1 and ϵ_2 are permittivities of the regions 1 and 2, respectively, the unit vector $\boldsymbol{n}$ normal to Γ' makes an angle θ with respect to the x-axis in the xy-plane, and the elements related to Γ' are grouped into two classes: the elements (e_1) in region 1 and the elements (e_2) in region 2.

If the functional for e_1 is used in its original form (14), we should modify the functional for e_2 in order to satisfy the boundary conditions of the electric field $\boldsymbol{E}$ on Γ'. For e_2, the functional (14) can be rewritten as

$$\tilde{F}_2 = \{E\}_2^T [A]_2 \{E\}_2 \tag{16a}$$

$$\{E\}_2 = \begin{bmatrix} \{E_x\}_2 \\ \{E_y\}_2 \\ \{E_z\}_2 \\ \{E_{x'}\}_2 \\ \{E_{y'}\}_2 \\ \{E_{z'}\}_2 \end{bmatrix} \tag{16b}$$

$$[A]_2 = \begin{bmatrix} [A_{xx}]_2 & [A_{xy}]_2 & [A_{xz}]_2 & [A_{xx'}]_2 & [A_{xy'}]_2 & [A_{xz'}]_2 \\ [A_{yx}]_2 & [A_{yy}]_2 & [A_{yz}]_2 & [A_{yx'}]_2 & [A_{yy'}]_2 & [A_{yz'}]_2 \\ [A_{zx}]_2 & [A_{zy}]_2 & [A_{zz}]_2 & [A_{zx'}]_2 & [A_{zy'}]_2 & [A_{zz'}]_2 \\ [A_{x'x}]_2 & [A_{x'y}]_2 & [A_{x'z}]_2 & [A_{x'x'}]_2 & [A_{x'y'}]_2 & [A_{x'z'}]_2 \\ [A_{y'x}]_2 & [A_{y'y}]_2 & [A_{y'z}]_2 & [A_{y'x'}]_2 & [A_{y'y'}]_2 & [A_{y'z'}]_2 \\ [A_{z'x}]_2 & [A_{z'y}]_2 & [A_{z'z}]_2 & [A_{z'x'}]_2 & [A_{z'y'}]_2 & [A_{z'z'}]_2 \end{bmatrix} \tag{16c}$$

where the components of the $\{E_i\}_2$ vector are the values of the electric field E_i $(i = x, y, z)$ at the nodal points within the element e_2 except Γ', the components of the $\{E_{i'}\}_2$ vector are the values of E_i at the nodal points on Γ' included in the element e_2, and the $[A_{xx}]_2$, $[A_{xy}]_2, \cdots,$ and $[A_{z'z'}]_2$ are the submatrices of the matrix (15) for e_2.

The tangential components of $\boldsymbol{E}$ and the normal component of $\epsilon_r \boldsymbol{E}$ should be continuous at the interface Γ'. These boundary conditions can be written as

$$\{E_{x'}\}_2 = q_{xx}\{E_{x'}\}_1 + q_{xy}\{E_{y'}\}_1 \tag{17a}$$

$$\{E_{y'}\}_2 = q_{xy}\{E_{x'}\}_1 + q_{yy}\{E_{y'}\}_1 \tag{17b}$$

$$\{E_{z'}\}_2 = \{E_{z'}\}_1 \tag{17c}$$

where the components of the $\{E_{i'}\}_1$ vector are the values of E_i at the nodal points on Γ' included in the element e_1, and q_{xx}, q_{xy}, and q_{yy} are given by

$$q_{xx} = \sin^2\theta + (\epsilon_1/\epsilon_2)\cos^2\theta \tag{18a}$$

$$q_{xy} = [(\epsilon_1/\epsilon_2) - 1]\sin\theta\cos\theta \tag{18b}$$

$$q_{yy} = \cos^2\theta + (\epsilon_1/\epsilon_2)\sin^2\theta. \tag{18c}$$

Using (17), (16) can be transformed as follows:

$$\tilde{F}_2 = \{\bar{E}\}_2^T [\bar{A}]_2 \{\bar{E}\}_2 \tag{19a}$$

$$\{\bar{E}\}_2 = \begin{bmatrix} \{E_x\}_2 \\ \{E_y\}_2 \\ \{E_z\}_2 \\ \{E_{x'}\}_1 \\ \{E_{y'}\}_1 \\ \{E_{z'}\}_1 \end{bmatrix} \tag{19b}$$

$$[\bar{A}]_2 = \begin{bmatrix} [A_{xx}]_2 & [A_{xy}]_2 & [A_{xz}]_2 & [\bar{A}_{xx'}]_2 & [\bar{A}_{xy'}]_2 & [A_{xz'}]_2 \\ [A_{yx}]_2 & [A_{yy}]_2 & [A_{yz}]_2 & [\bar{A}_{yx'}]_2 & [\bar{A}_{yy'}]_2 & [A_{yz'}]_2 \\ [A_{zx}]_2 & [A_{zy}]_2 & [A_{zz}]_2 & [\bar{A}_{zx'}]_2 & [\bar{A}_{zy'}]_2 & [A_{zz'}]_2 \\ [\bar{A}_{x'x}]_2 & [\bar{A}_{x'y}]_2 & [\bar{A}_{x'z}]_2 & [\bar{A}_{x'x'}]_2 & [\bar{A}_{x'y'}]_2 & [\bar{A}_{x'z'}]_2 \\ [\bar{A}_{y'x}]_2 & [\bar{A}_{y'y}]_2 & [\bar{A}_{y'z}]_2 & [\bar{A}_{y'x'}]_2 & [\bar{A}_{y'y'}]_2 & [\bar{A}_{y'z'}]_2 \\ [A_{z'x}]_2 & [A_{z'y}]_2 & [A_{z'z}]_2 & [\bar{A}_{z'x'}]_2 & [\bar{A}_{z'y'}]_2 & [A_{z'z'}]_2 \end{bmatrix} \tag{19c}$$

where

$$[\bar{A}_{x'x'}]_2 = q_{xx}^2[A_{x'x'}]_2 + q_{xx}q_{xy}([A_{x'y'}]_2 + [A_{y'x'}]_2) + q_{xy}^2[A_{y'y'}]_2 \tag{20a}$$

$$[\bar{A}_{x'y'}]_2 = q_{xx}q_{xy}[A_{x'x'}]_2 + q_{xx}q_{yy}[A_{x'y'}]_2 + q_{xy}^2[A_{y'x'}]_2 + q_{xy}q_{yy}[A_{y'y'}]_2 \tag{20b}$$

$$[\bar{A}_{y'x'}]_2 = q_{xx}q_{xy}[A_{x'x'}]_2 + q_{xx}q_{yy}[A_{y'x'}]_2 + q_{xy}^2[A_{x'y'}]_2 + q_{xy}q_{yy}[A_{y'y'}]_2 \tag{20c}$$

$$[\bar{A}_{y'y'}]_2 = q_{xy}^2[A_{x'x'}]_2 + q_{xy}q_{yy}([A_{x'y'}]_2 + [A_{y'x'}]_2) + q_{yy}^2[A_{y'y'}]_2 \tag{20d}$$

$$[\bar{A}_{jx'}]_2 = q_{xx}[A_{jx'}]_2 + q_{xy}[A_{jy'}]_2, \qquad j = x, y, z, z' \tag{20e}$$

$$[\bar{A}_{jy'}]_2 = q_{xy}[A_{jx'}]_2 + q_{yy}[A_{jy'}]_2, \qquad j = x, y, z, z' \tag{20f}$$

$$[\bar{A}_{x'j}]_2 = q_{xx}[A_{x'j}]_2 + q_{xy}[A_{y'j}]_2, \qquad j = x, y, z, z' \tag{20g}$$

$$[\bar{A}_{y'j}]_2 = q_{xy}[A_{x'j}]_2 + q_{yy}[A_{y'j}]_2, \qquad j = x, y, z, z'. \tag{20h}$$

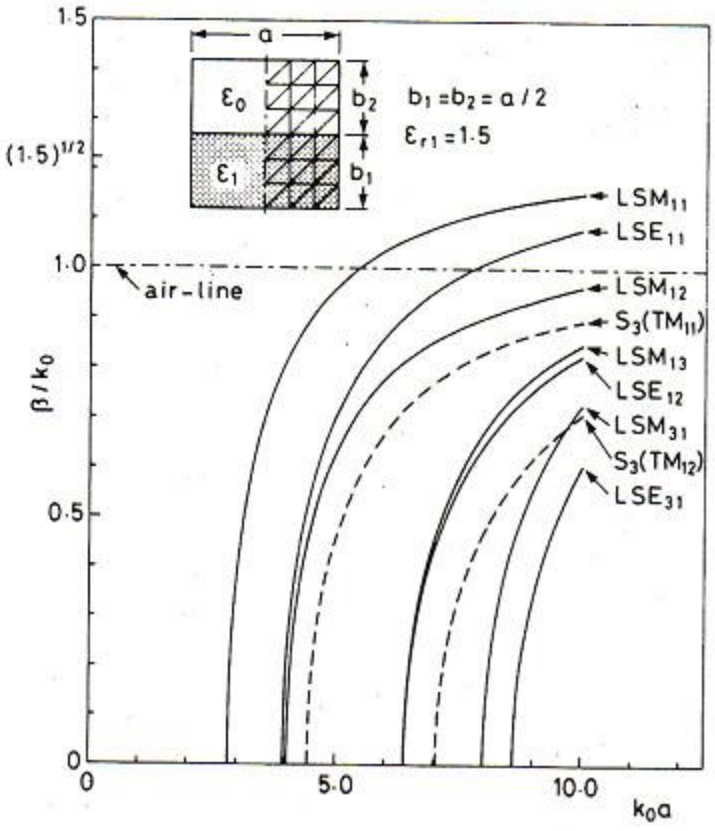

Fig. 2. Dispersion characteristics of a half-filled dielectric waveguide.

By using the original functional (14) for e_1 and the modified functional (19) for e_2, the boundary conditions of the electric field $\boldsymbol{E}$ at the interface with an abrupt discontinuity in the permittivity are satisfied.

IV. Numerical Results

A. Dielectric-Loaded Waveguides

First, let us consider a rectangular waveguide half-filled with a dielectric of permittivity ϵ_1 (relative permittivity $\epsilon_{r1} = \epsilon_1/\epsilon_0$).

We subdivide one half of the cross section into second-order triangular elements as shown in the insert in Fig. 2, where $\epsilon_{r1} = 1.5$, the plane of symmetry is assumed to be a perfect magnetic conductor, 36 elements (N_E) are used, and the number of the nodal points (N_p) is 91. Computed results (solid lines) for the LSM_{mn} and LSE_{mn} modes agree well with the exact results [16]. Spurious solutions S_1 and S_2, which are included in (5), do not appear. Spurious solutions S_3 (dashed lines) corresponding to the solutions of (12) appear only in the region $\beta/k_0 < 1$. The solutions S_3 with cutoff frequencies $k_0a = \sqrt{2}\,\pi$ and $\sqrt{5}\,\pi$ are equivalent to the TM_{11} and TM_{12} modes of a "hollow" waveguide of square cross section, respectively.

One can control the solutions S_3 by changing the functional (8) as follows [10], [15]:

$$\tilde{F}_p = \iint_\Omega (\nabla \times \boldsymbol{E})^* \cdot \left([\mu_r]^{-1} \nabla \times \boldsymbol{E}\right) d\Omega - k_0^2 \iint_\Omega \epsilon_r \boldsymbol{E}^* \cdot \boldsymbol{E}\, d\Omega + p^2 \iint_\Omega \epsilon_r^{-1} (\nabla \cdot \epsilon_r \boldsymbol{E})^* (\nabla \cdot \epsilon_r \boldsymbol{E})\, d\Omega \qquad (21)$$

where p is a positive number. If p is set equal to 1, $\tilde{F}_p$ becomes $\tilde{F}$. For (21), (12) is reduced to

$$(p^2 \nabla^2 + k_0^2)\psi = 0 \quad \text{in region } \Omega \qquad (22a)$$

$$\psi = 0 \quad \text{on perfect electric conductor} \qquad (22b)$$

$$\partial\psi/\partial n = 0 \quad \text{on perfect magnetic conductor.} \qquad (22c)$$

The appearance of the solutions of (22) is limited to the region $\beta/k_0 < 1/p$ and the cutoff frequencies of these solutions vary in proportion to the value of p.

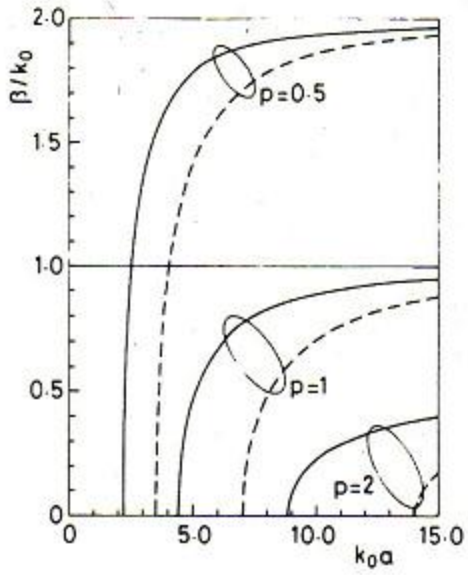

Fig. 3. p-dependence for the spurious solutions S_3.

Fig. 3 shows the p-dependence for the solutions S_3 in the same waveguide as shown in Fig. 2. Solid and dashed lines in Fig. 3 correspond to the TM_{11} and TM_{12} modes in Fig. 2, respectively. When $p = 2$, the solutions S_3 appear in the region $\beta/k_0 < 0.5$ and the cutoff frequencies of the solutions corresponding to the TM_{11} and TM_{12} modes in Fig. 2 become $k_0a = 2\sqrt{2}\,\pi$ and $2\sqrt{5}\,\pi$, respectively. When $p = 0.5$, the solutions S_3 appear in the region $\beta/k_0 < 2$ and the cutoff frequencies of the solutions corresponding to the TM_{11} and TM_{12} modes in Fig. 2 become $k_0a = 0.5\sqrt{2}\,\pi$ and $0.5\sqrt{5}\,\pi$, respectively. The p-dependence is very small for the physical solutions. For larger values of p, however, the degree of accuracy for the physical solutions becomes poorer. For smaller values of p, on the other hand, more spurious solutions appear, because the cutoff frequencies of these spurious solutions become lower. Hereafter, we use $p = 1$, namely the functional (8).

Fig. 4 shows the dispersion characteristics for the fundamental mode of half-filled dielectric waveguides, where the plane of symmetry is assumed to be a perfect magnetic conductor. For both $\epsilon_{r1} = 1.5$ and 10.0, our results agree well with the results of the $\boldsymbol{H}$-field finite-element formulation [11].

In Figs. 2 and 4, the normal direction of the interface with an abrupt change in the permittivity coincides with the direction of a coordinate axis.

Next, let us consider a rectangular waveguide with a diamond-shaped dielectric insert [17], as shown in Fig. 5. In this waveguide, there are abrupt changes in the permittivity at the interface whose normal direction does not coincide with the direction of a coordinate axis. Fig. 5 shows the dispersion characteristics for the fundamental

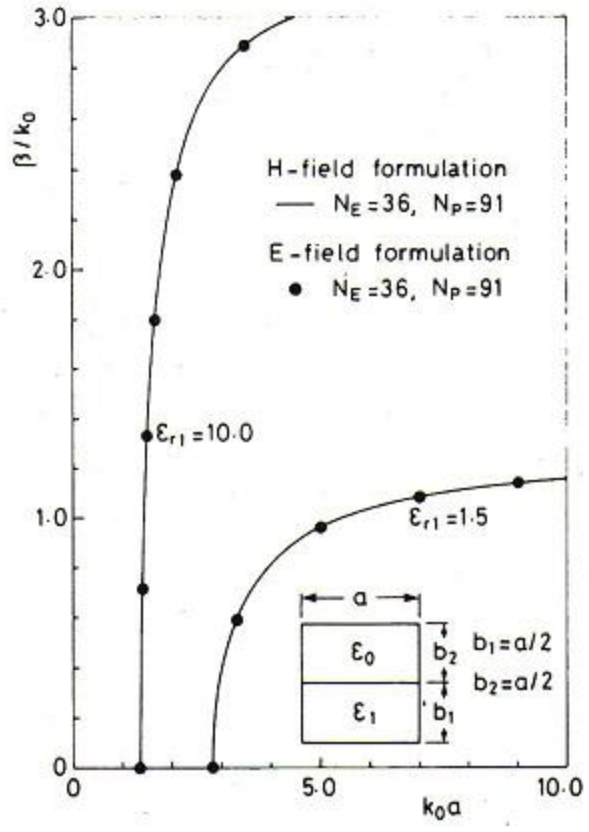

Fig. 4. Dispersion characteristics for the fundamental mode of half-filled dielectric waveguides.

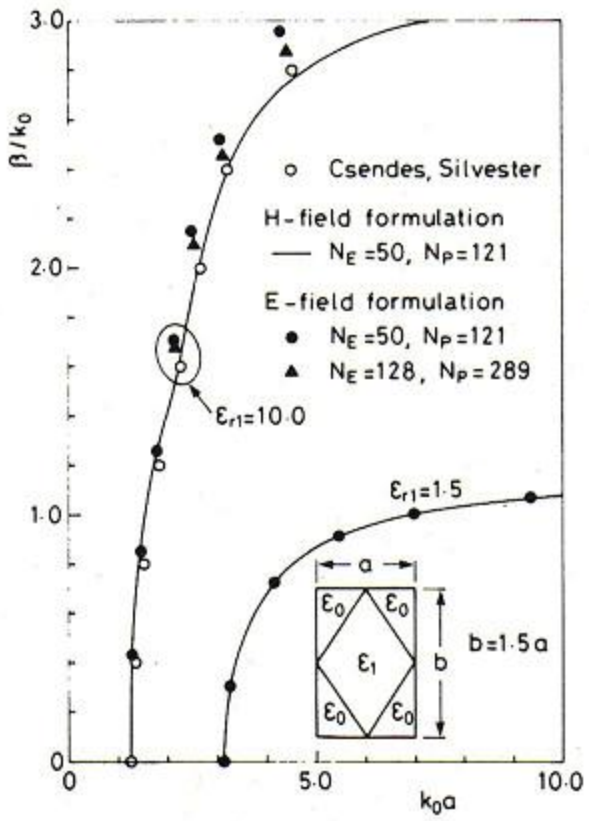

Fig. 5. Dispersion characteristics for the fundamental mode of rectangular waveguides with a diamond-shaped dielectric insert.

mode, where two planes of symmetry are assumed to be perfect magnetic conductors and one quarter of the cross section is divided into second-order triangular elements. In Fig. 5, the results of the ***H***-field formulation with $N_E = 50$ and $N_P = 121$ and the results of the modal approximation techniques [17] are also presented. For $\epsilon_{r1} = 1.5$, the results of the ***E***-field formulation with $N_E = 50$ and $N_P = 121$ agree well with those of the ***H***-field formulation. For a larger value of relative permittivity, $\epsilon_{r1} = 10.0$, the results of the ***E***-field formulation with $N_E = 50$ and $N_P = 121$ deviate from those of the ***H***-field formulation at higher frequencies. However, the ***E***-field finite-element solutions can be improved by increasing the number of the elements. The results of the ***E***-field formulation with $N_E = 128$ and $N_P = 289$ are closer to those of the ***H***-field formulation.

The computed results in Figs. 2, 4, and 5 prove the validity of (19) and (20).

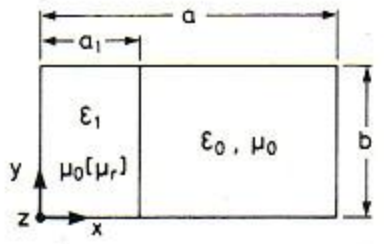

Fig. 6. Ferrite-loaded waveguide.

TABLE I
DISPERSION CHARACTERISTICS OF FERRITE-LOADED WAVEGUIDES

βb	$k_0 b$			
	$a_1 = a$		$a_1 = a/4$	
	Finite-element calculation	Exact calculation	Finite-element calculation	Exact calculation
-1	0.78877	0.78876	1.45379	1.45364
0	0.66538	0.66537	1.16095	1.16087
1	0.78877	0.78876	1.39979	1.39966

B. Ferrite-Loaded Waveguides

We consider a ferrite-loaded waveguide as shown in Fig. 6. The ferrite material is characterized by the relative permeability tensor

$$[\mu_r] = \begin{bmatrix} 3.0 & 0 & j0.8 \\ 0 & 1.0 & 0 \\ -j0.8 & 0 & 3.0 \end{bmatrix} \tag{23}$$

and a relative permittivity of 2.0 [5]. Here, $[\mu_r]$ is independent of frequency, although this assumption is not valid for ferrites in general [5]. Table I shows the dispersion characteristics for the fundamental mode, where $a = 2b$, $N_E = 64$, and $N_p = 153$. For both $a_1 = a$ (completely filled) and $a_1 = a/4$, agreement between our results and the exact results [5], [18] is good. In the case of $a_1 = a/4$, the value of $k_0 b$ for $\beta b = -1$ is different from that for $\beta b = 1$. This fact implies that when k_0 is given, the modes propagating in this structure (partially filled) in the opposite directions have different phase constants, namely these modes are nonreciprocal [18]. The modes propagating in the completely filled waveguide in the opposite directions, on the other hand, have the same phase constants, and therefore, these modes are reciprocal [18].

V. CONCLUSION

The finite-element method was formulated for the analysis of anisotropic waveguides with a nondiagonal permeability tensor in terms of all three components of the electric field ***E***. In this approach, spurious solutions do not appear anywhere above the "air-line." The application of this ***E***-field formulation to waveguides with an abrupt discontinuity in the permittivity was discussed in detail.

REFERENCES

[1] P. Daly, "Hybrid-mode analysis of microstrip by finite-element methods," *IEEE Trans. Microwave Theory Tech.*, vol. MTT-19, pp. 19–25, Jan. 1971.

[2] M. Ikeuchi, H. Sawami, and H. Niki, "Analysis of open-type dielectric waveguides by the finite-element iterative method," *IEEE Trans. Microwave Theory Tech.*, vol. MTT-29, pp. 234–239, Mar. 1981.
[3] N. Mabaya, P. E. Lagasse, and P. Vandenbulcke, "Finite element analysis of optical waveguides," *IEEE Trans. Microwave Theory Tech.*, vol. MTT-29, pp. 600–605, June 1981.
[4] K. Oyamada and T. Okoshi, "Two-dimensional finite-element calculation of propagation characteristics of axially nonsymmetrical optical fibers," *Radio Sci.*, vol. 17, pp. 109–116, Jan.–Feb. 1982.
[5] A. Konrad, "High-order triangular finite elements for electromagnetic waves in anisotropic media," *IEEE Trans. Microwave Theory Tech.*, vol. MTT-25, pp. 353–360, May 1977.
[6] B. M. A. Rahman and J. B. Davies, "Finite-element analysis of optical and microwave waveguide problems," *IEEE Trans. Microwave Theory Tech.*, vol. MTT-32, pp. 20–28, Jan. 1984.
[7] M. Hano, "Finite-element analysis of dielectric-loaded waveguides," *IEEE Trans. Microwave Theory Tech.*, vol. MTT-32, pp. 1275–1279, Oct. 1984.
[8] M. Koshiba, K. Hayata, and M. Suzuki, "Vectorial finite-element formulation without spurious modes for dielectric waveguides," *Trans. Inst. Electron. Commun. Eng. Japan*, vol. E67, pp. 191–196, Apr. 1984.
[9] M. Koshiba, K. Hayata, and M. Suzuki, "Vectorial finite-element method without spurious solutions for dielectric waveguide problems," *Electron. Lett.*, vol. 20, pp. 409–410, May 1984.
[10] B. M. A. Rahman and J. B. Davies, "Penalty function improvement of waveguide solution by finite elements," *IEEE Trans. Microwave Theory Tech.*, vol. MTT-32, pp. 922–928, Aug. 1984.
[11] M. Koshiba, K. Hayata, and M. Suzuki, "Improved finite-element formulation in terms of the magnetic-field vector for dielectric waveguides," *IEEE Trans. Microwave Theory Tech.*, vol. MTT-33, pp. 227–233, Mar. 1985.
[12] A. Konrad, "Vector variational formulation of electromagnetic fields in anisotropic media," *IEEE Trans. Microwave Theory Tech.*, vol. MTT-24, pp. 553–559, Sept. 1976.
[13] A. D. Berk, "Variational principle for electromagnetic resonators and waveguides," *IRE Trans. Antennas Propagat.*, vol. AP-4, pp. 104–111, Apr. 1956.
[14] J. B. Davies, F. A. Fernandez, and G. Y. Philippou, "Finite element analysis of all modes in cavities with circular symmetry," *IEEE Trans. Microwave Theory Tech.*, vol. MTT-30, pp. 1975–1980, Nov. 1982.
[15] M. Hara, T. Wada, T. Fukasawa, and F. Kikuchi, "A three dimensional analysis of RF electromagnetic fields by the finite element method," *IEEE Trans. Magn.*, vol. MAG-19, pp. 2417–2420, Nov. 1983.
[16] N. Marcuvitz, *Waveguide Handbook*. New York: McGraw-Hill, 1951.
[17] Z. J. Csendes and P. Silvester, "Numerical solution of dielectric loaded waveguides: II—Modal approximation technique," *IEEE Trans. Microwave Theory Tech.*, vol. MTT-19, pp. 504–509, June 1971.
[18] B. Lax and K. J. Button, "Theory of new ferrite modes in rectangular wave guide," *J. Appl. Phys.*, vol. 26, pp. 1184–1185, Sept. 1955.

Masanori Koshiba (SM'84) was born in Sapporo, Japan, on November 23, 1948. He received the B.S., M.S., and Ph.D. degrees in electronic engineering from Hokkaido University, Sapporo, Japan, in 1971, 1973, and 1976, respectively.

In 1976, he joined the Department of Electronic Engineering, Kitami Institute of Technology, Kitami, Japan. Since 1979, he has been an Assistant Professor of Electronic Engineering at Hokkaido University. He has been engaged in research on surface acoustic waves, dielectric optical waveguides, and applications of finite-element and boundary-element methods to field problems.

Dr. Koshiba is a member of the Institute of Electronics and Communication Engineers of Japan, the Institute of Television Engineers of Japan, the Institute of Electrical Engineers of Japan, the Japan Society for Simulation Technology, and Japan Society for Computational Methods in Engineering.

✠

Kazuya Hayata was born in Kushiro, Japan, on December 1, 1959. He received the B.S. and M.S. degrees in electronic engineering from Hokkaido University, Sapporo, Japan, in 1982 and 1984, respectively.

Since 1984, he has been a Research Assistant of Electronic Engineering at Hokkaido University. He has been engaged in research on dielectric optical waveguides and surface acoustic waves.

Mr. Hayata is a member of the Institute of Electronics and Communication Engineers of Japan.

✠

Michio Suzuki (SM'57) was born in Sapporo, Japan, on November 14, 1923. He received the B.S. and Ph.D. degrees in electrical engineering from Hokkaido University, Sapporo, Japan, in 1946 and 1960, respectively.

From 1948 to 1962, he was an Assistant Professor of Electrical Engineering at Hokkaido University. Since 1962, he has been a Professor of Electronic Engineering at Hokkaido University. From 1956 to 1957, he was a Research Associate at the Microwave Research Institute of the Polytechnic Institute of Brooklyn, Brooklyn, NY.

Dr. Suzuki is a member of the Institute of Electronics and Communication Engineers of Japan, the Institute of Electrical Engineers of Japan, the Institute of Television Engineers of Japan, the Japan Society of Information and Communication Research, and the Japan Society for Simulation Technology.